

1

Are Covalent Bonds really Directed?

I. David Brown

Brockhouse Institute for Materials Research, McMaster University, Hamilton, ON, Canada L8S

4M1.

idbrown@mcmaster.ca

Abstract

The flux theory of the chemical bond, which provides a physical description of chemical structure based on classical electrostatic theory, correctly predicts the angles between bonds, to the extent that they depend on the intrinsic properties of the bonded atoms. It is based on the justifiable assumption that the charge density around the nucleus of an atom retains most of its spherical symmetry even when bonded. A knowledge of these intrinsic bond angles permits the measurement and analysis of the steric angular strains that result from the mapping of the bond network into three dimensional space. The work ends by pointing out that there are better ways of characterizing bonds than describing them as covalent or ionic.

Keywords

Bond angles

Flux bonding theory

Directed bonds

Introduction

It is often said that ‘covalent bonds are directed but ionic bonds are not’. This is presented as if it were a profound observation about the nature of chemical bonding, but it

23 depends on the questionable assumption that bonds can be neatly divided into two clearly
24 distinguishable classes, covalent and ionic, even though it is widely accepted that bonds lie on a
25 single continuum and such a distinction is difficult to make.

26 The purpose of this paper is to examine to what extent bonds can be said to be directed.
27 Using the flux theory of the chemical bond, more fully described by Brown (2014a), it argues
28 that bond directions are determined by the spherical symmetry of the atoms and no distinction
29 needs to be made between bonds of different character. The flux theory is first briefly reviewed
30 as it involves few if any of the concepts commonly used to describe chemical bonding.

31 **The flux theory of the chemical bond**

32 For many years it has been fashionable to discuss chemical bonding as a quantum
33 phenomenon, but the idea of a chemical bond predates quantum mechanics by half a century; its
34 properties are rooted in classical physics, yet in our search for a quantum explanation of bonding
35 we have failed to appreciate the extent to which classical electrostatic theory gives a physically
36 correct description of the chemical structures formed by the quantum atom. While there is no
37 doubt that quantum mechanics is essential for understanding atomic spectra, chemical structure
38 generally involves only the ground state of the atom so that the greater part of structure theory is
39 readily derived using only classical electrostatics. The key is to recognize that the chemical
40 bond and the electrostatic flux have the same properties. Both depend only on the amount of
41 charge (the valence) that is used to form the bond and neither depends on where that charge is
42 located. This contrasts with quantum mechanical descriptions, which supply exactly the
43 information that the bond theory does not require. Quantum mechanics accurately describes the
44 location of the charge between the atoms, but is unable to identify how much charge is used to

45 form a given bond. Quantum mechanics cannot be entirely ignored in such a classical approach,
46 but in most cases the essential constraints that it describes can easily be introduced via a few
47 plausible ad hoc rules and a small number of empirically determined atomic and bond
48 parameters. This is not to say that quantum calculations do not properly describe chemical
49 bonding, only that the flux picture provides a complementary, simpler, yet physically accurate
50 picture that has many advantages in predicting structure and geometry. This section describes the
51 features of the flux model that are necessary to understand how the flux can be used to
52 determined bond angles. It is a particularly simple theory because it uses only concepts that are
53 introduced early into the physics curriculum at about the same time that the chemical curriculum
54 introduces the concept of the chemical bond.

55 An important heuristic that underlies the flux theory of the chemical bond is the principle
56 of maximum symmetry which states that:

57 A system in stable static equilibrium adopts the highest symmetry that is consistent with
58 the constraints acting on it (Brown 2009). (1)

59 The justification for this principle is that the presence of a symmetry element in such a system is
60 necessarily an energy minimum with respect to any deformation of the system that breaks this
61 symmetry. By definition, a system in stable static equilibrium is at an energy minimum, and
62 displacing an atom in such a system from a mirror plane (for example) in either direction must
63 result in an increase in the energy. An equilibrium system with mirror symmetry has a lower
64 energy than the same system in which this mirror plane is lost, unless there is some physical
65 constraint that prevents the system from adopting the mirror symmetry. A corollary of this
66 principle is:

67 If a system lacks a potential symmetry element, a constraint that breaks that symmetry
68 must be present. (2)

69 The electrostatic flux that lies at the heart of the theory is the same as the number of
70 Faraday lines of electric field that link two equal and opposite charges. It is scaled so that the
71 flux is equal in magnitude to each of these charges, and if each line of field represents one unit of
72 charge, the flux is equal to the total number of lines linking the charges. The unit in which the
73 charge and flux are measured in this theory is the valence unit (vu) which is equal to the charge
74 of one electron. The valence of an atom is defined as the amount of charge the atom uses for
75 bonding.

76 An atom consists of a nucleus surrounded by a cloud of negative charge whose density
77 can be calculated from quantum mechanics. Although the charge surrounding the nucleus is
78 often described as being composed of discrete electrons, individual electrons can be neither
79 identified nor located in the atom; the electron as an entity disappears as soon as it enters the
80 atom, but it bequeaths its charge, spin and mass to the charge cloud of the atom. For this
81 reason the term ‘charge density’ is preferred to the more usual term ‘electron density’.

82 Because the flux does not depend on the location of the charge, details of the radial
83 distribution of the charge density are irrelevant in the flux theory. However, for the calculation
84 of angles it is important that the flux have spherical symmetry. For the free atom spherical
85 symmetry follows from the principle of maximum symmetry, but the strong central force of the
86 nucleus ensures that the charge density remains essentially spherical even when the atom is
87 bonded. Although on bond formation the charge density relaxes in important ways, the density
88 typically changes by only a few percent. While this results in significant changes to the energy,

89 the difference it makes to the flux description of the bond is small and unimportant. The
90 assumption of spherical symmetry, and a consideration of where this spherical symmetry might
91 be violated, is central to the prediction of bond angles.

92 <Figure 1 >

93 For atoms with atomic numbers less than 18 (argon) the ionization energies identify a
94 shell of charge (known as the valence shell) that is bound sufficiently weakly to be available to
95 form chemical bonds. This shell carries a negative charge which is linked to the positively
96 charged core by an electrostatic flux equal to the amount of charge in the valence shell. Fig. 1
97 shows a schematic picture of two bonded atoms. The valence shell (gray) of each atom is
98 shown as separated from its respective core (light gray) so as to leave room to display the flux
99 lines (arrows) that link the valence shell to the core. This schematic separation is permitted,
100 because although in the physical atom the core and valence shell overlap, the flux does not
101 depend on where the charges are physically located.

102 When two atoms form a bond, their valences shells overlap as shown conceptually by the
103 black region in Fig. 1, each atom retaining spherical symmetry and contributing equal amounts
104 of charge to the bond. The flux that forms the bond is shown by the solid arrows linking the core
105 of each atom to the valence charge that each atom contributes to the bond.

106 The overlap between the two valence shells occurs at some point along the line joining
107 the two nuclei, but since the flux does not depend on where this point occurs we are free to
108 imagine the overlapping bonding charge lying at any convenient point. We can assume that it
109 lies at the center of the bond, or if it proves more useful, we can assume that all the bonding
110 charge lies within the boundary of either of the two bonded atoms. Whichever choice we make,

111 the flux is the same, but the different choices lead to different bond models. If we assume that
112 the overlap occurs in the middle of the bond we have the *neutral atom model* in which we assign
113 each portion of the bonding charge to its own atom. This is the situation shown in Fig. 1.¹
114 Alternatively, if we assign all the bonding charge to the atom that we call the anion, we have
115 created the *ionic model* in which the flux lines run from the cations to the anions. Restricting
116 bonds to those with integral valence leads to the VSEPR model discussed in Section 6 as well as
117 the ball-and-stick model of organic chemistry. Because the flux is independent of the actual
118 location of the charge, all these models can be used to describe any bond, regardless of where the
119 bonding charge might physically be located, subject only to any assumptions that restrict the
120 scope of the model. For example, the ionic model can be used to describe covalent structures
121 such as the acetate ion (Brown 1980), subject only to the topological restriction that every bond
122 must have an atom labelled ‘anion’ at one end and an atom labelled ‘cation’ at the other; the
123 ionic model cannot be used to describe cation-cation or anion-anion bonds. This restriction is
124 mathematical not chemical, so the anion electronegativity need not be larger than that of the
125 cation. The neutral atom model can be used to describe any localized bond, but the ionic model
126 leads to more useful theorems.

127 The closer two atoms are brought together, the greater the amount of charge in the bond
128 overlap region and the greater the flux forming the bond. The length of the bond thus correlates
129 with the amount of flux in the bond, but it also depends on the sizes of the atoms. The size does
130 require a knowledge of the radial distribution of the charge of each atom and can only be

¹ Fig. 1 shows only one bonded atom. In crystals each atom is surrounded by other atoms so all the valence shell charge is used for bonding. However, the presence of non-bonding charge (lone pairs) in the valence shell prevents the formation of bonds in some directions resulting in the creation of molecules (see Sections 6 and 7).

131 calculated using quantum mechanics, so in the flux theory the correlation between the length, R_{ij} ,
132 and the flux, ϕ_{ij} (or valence,² s_{ij}) of the bond between atoms i and j is determined empirically
133 from crystal structure determinations. This correlation can be described for most bond types by
134 the simple expression given in eqn (3), whose two empirical parameters, R_0 and b , are tabulated
135 for many bond types (Brown 2014b) and are robustly transferable among all bonds between the
136 same pair of atoms.

$$137 \quad s_{ij} = \exp((R_0 - R_{ij})/b) \quad (3)$$

138 Since the valence of an atom is the total amount of charge it uses to form all its bonds, it
139 follows that the sum of the fluxes, ϕ_{ij} (or valences, s_{ij}) of all the bonds formed by atom i must be
140 equal to its atomic valence, V_i . The valence sum rule, eqn (4), is the central rule of the flux
141 theory.

$$142 \quad V_i = \sum_j \phi_{ij} = \sum_j s_{ij} \quad (4)$$

143 In the ionic version of the flux theory a chemical bond is an electric capacitor since it
144 consists of two equal and opposite charges (on the cation and the anion) linked by electrostatic
145 flux. A bond network is therefore a capacitive electrical circuit. It can be solved using the two
146 Kirchoff equations provided the capacitance of each bond is known. The bond capacitance
147 cannot be calculated from first principles, but in the absence of any constraint that might destroy
148 the intrinsic equivalence of all the bonds, the principle of maximum symmetry implies that all
149 bonds should have the same capacitance. If the capacitances are all the same they cancel from

² The bond flux and bond valence are two different names for the same concept. The term ‘bond flux’, ϕ , is normally used for the theoretically determined flux, ‘bond valence’, s , is used for the same quantity when determined experimentally. The distinction is convenient when comparing theoretically predicted values with the experimentally determined values which are subject to experimental uncertainty.

150 the Kirchhoff equations, yielding the set of network equations (5) and (6) from which the bond
151 fluxes can be predicted (Brown 2002).

$$152 \quad V_i = \sum_j \phi_{ij} \quad (5)$$

$$153 \quad 0 = \sum_{\text{loop}} \phi_{ij} \quad (6)$$

154 Once the fluxes are known, bond lengths can be predicted using eqn (3) with ϕ
155 substituted for s . In the absence of any constraint arising from electronic anisotropies (Sections 7
156 and 8) or steric stresses (discussed in Section 9), the bond lengths predicted this way agree with
157 experiment to within a few hundredths of an Ångström (Preiser et al. 1999). These predictions
158 of bond lengths can be made from a knowledge of only the bond topology; it is not necessary to
159 know the spatial arrangement of the atoms in three-dimensions.

160 The ion, i , can be characterized by its bonding strength, S_i , which is defined by eqn (7),
161 where $\langle N \rangle_i$ is a typical coordination number for atom i , conveniently taken as the average
162 coordination number formed with oxygen (Brown, 1988).

$$163 \quad S_i = V_i / \langle N \rangle_i \quad (7)$$

164 The bonding strengths given by Brown (2014a) are a measure of the flux of a typical bond
165 formed by the atom. It is convenient to distinguish between the bonding strength of a cation, S_A
166 (A for Lewis acid) and the bonding strength of an anion, S_B , (B for Lewis base), S_A often being
167 shown with a plus sign and S_B with a minus sign. For example, the bonding strength, S_A , of the
168 magnesium ion is $+2/6 = +0.33$ valence units (vu), while that for the sulfur ion is $+6/4 = +1.50$
169 vu. S_B for oxygen is $-2/4 = -0.50$ vu. Since the bonding strength is an estimate of the flux of a
170 typical bond formed by an atom, one expects stable bonds to be formed only between atoms with
171 similar bonding strengths. The condition for bond formation is given by eqn (8), known as the

172 valence matching rule.

$$173 \quad 0.5 < |S_A/S_B| < 2 \quad (8)$$

174 In many cases eqn (8) is sufficient to determine the bond network from which bond lengths can
175 be predicted. This summary provides the essential background needed to understand how the
176 flux theory can be used to determine the bond angles.

177 **Using the flux theory to predict bond directions**

178 The following assumption is central to the use of the flux theory in the prediction of bond
179 angles.

$$180 \quad \textit{Atoms are spherically symmetric even when they are bonded to other atoms.} \quad (9)$$

181 The justification for this assumption is given in Section 2. If the negative charge of an atom is
182 distributed around the nucleus with spherical symmetry, the flux linking the core and the valence
183 shell must also be spherically symmetric as shown in Fig. 1. Although the flux of a bond does
184 not depend on the radial distribution of the charge around the atom, its direction does depend on
185 its angular distribution. It follows from the assumption (9) that the solid angle subtended by a
186 bond at the nucleus of a spherical atom is proportional to its flux as given by eqn (10):

$$187 \quad \Omega_{ij} = 4\pi(\phi_{ij}/V_i) = 4\pi(s_{ij}/V_i) \quad (10)$$

188 where Ω_{ij} is the solid angle in steradians at atom i subtended by the bond of flux, ϕ_{ij} , (or valence,
189 s_{ij}). 4π is the solid angle of the whole sphere. This is the relation that determines the bond
190 angles.

191 Converting the solid angle subtended by a bond into the angle between two bonds is,
192 however, not straightforward. Complications arise on two accounts. The geometric problem of
193 converting solid angles into bond angles, and the presence of additional constraints, either

194 electronic or steric, that lower the symmetry in the coordination sphere of the central atom.

195 Each of these problems is addressed below.

196 **High symmetry structures**

197 The simplest cases are easy to deal with. If all the bonds formed by an atom have the
198 same bond flux, the principle of maximum symmetry implies that, if possible, all these bonds
199 will be related by symmetry. Two bonds will be collinear, three will point to the corners of a
200 triangle, four to the corners of a tetrahedron and six to the corners of an octahedron. There is no
201 reasonable coordination geometry in which five or seven bonds can all be related by symmetry.
202 This explains the frequency with which tetrahedral and octahedral coordination are found while
203 five and seven coordination are adopted only when constraints make four or six coordination
204 impossible. The high symmetry coordination spheres that make the bonds equivalent
205 automatically determine the bond angles. The principle of maximum symmetry, eqn (1),
206 accounts for most of the observed coordination geometries without the need to distinguish
207 between covalent and ionic bonds. The hybrid orbitals that are often presumed to determine
208 covalent bond directions merely reflect the possible high symmetry point groups with two, three
209 and four-fold symmetry, but for light atoms, hybrid orbitals are unable to account for the six-fold
210 coordination found around the cations in, e.g., Al_2O_3 , PF_6^- and SF_6 .³ The problem of
211 hypervalency that arises in orbital models does not exist in the flux theory.

212 **Lowering the symmetry, the influence of the bond network**

213 In some compounds the presence of additional constraints results in the breaking of the

³ There are many other problems with the hybridized orbital model. The spherical harmonics used to describe the orbitals are not wave functions, just a mathematical tool rather than a physical concept. A filled set of s-p orbitals in any hybridized form has, by definition, perfect spherical symmetry, favoring no particular directions.

214 high symmetries described in Section 4. Three constraints can be identified. A lower
215 symmetry may be imposed either by the bond network (Section 5), the electronic structure of the
216 atom (Sections 6-8), or by three dimensional space (Section 9).

217 If the bonded neighbors of an atom have different environments in the bond network they
218 may have different fluxes, in which case the solid angles subtended by the bonds will not be
219 equal. Eqn (10) still applies: stronger bonds will subtend larger angles. Consequently we
220 expect the bond angles formed between stronger bonds to be larger than those between weaker
221 bonds. The difficulty arises in converting the solid angles into angles between the bonds. A
222 couple of techniques are available for making these predictions quantitative as illustrated by the
223 following examples.

224 The X_2O_7 complexes (most of them anions), where $X = Si^{4+}$, P^{5+} , S^{6+} and Cl^{7+} , consist
225 of two tetrahedra sharing a common bridging oxygen atom, O_b . The remaining six oxygen
226 atoms within the complex are terminal, O_t , but if the complex is an anion the terminal oxygen
227 atoms will also form weak bonds to external cations. The angles of interest are the O_t-X-O_t and
228 O_t-X-O_b angles within the tetrahedron, and the $X-O_b-X$ angle at the bridging oxygen that links
229 the two tetrahedra. The latter angle is of particular interest in the mineralogy of silicate
230 minerals as they link the SiO_4 tetrahedra into chain-, sheet- and framework-minerals (Gibbs et al.
231 1972). These $X-O_b-X$ angles are discussed in Section 7.

232 Since the behavior of the O-X-O angles of all these complexes is the same, the discussion
233 here is limited to the case where X is S^{6+} . The bond fluxes can be predicted using the network
234 equations (5) and (6), but in the case where the S- O_t bonds are all equivalent the fluxes can be
235 assigned by inspections. Since the valence sums at S and O_b must equal the atomic valence, the

236 flux of each of the two S-O_b bonds is 1.00 vu, hence that of the S-O_t bonds is 1.67 vu. From eqn
237 (10) it is clear that the O_t-S-O_t angle must be greater than 109° and that the O_t-S-O_b angle must be
238 correspondingly smaller. These estimates can be made quantitative in two different ways, the
239 difficulty lies in how to convert the solid angles, which can cover the sphere in different ways,
240 into the angles between bonds.

241 <Table 1 here>

242 The first approach to calculating these angles was proposed by Murray-Rust et al. (1975)
243 and Brown (1980b). A correlation between the bond angle and the average valence of the two
244 bonds that defines the angle is found by interpolating between two limiting configurations in
245 which the angles are defined by symmetry. In the present case one of these is the regular SO₄
246 tetrahedron in which the four S-O bonds each have a flux of 1.50 vu and the angle between them
247 is 109°. The other limiting configuration is the planar SO₃ triangle that would be obtained by
248 removing the bridging oxygen, O_b, to infinity. In the latter case the bond fluxes are 2.00 vu for
249 the three S-O_t bonds and 0 vu for the S-O_b bond, with an O_t-S-O_t angle of 120° and an O_t-S-O_b
250 angle of 90°. A second order fit (eqn (11)) between the average fluxes of the bond pairs, s , and
251 these three angles, θ , yields the predictions shown in column 2 of Table 1.

$$252 \quad \theta = 46(\varphi-1) - 16(\varphi-1)^2 + 90 \quad (11)$$

253 An alternative approach, proposed independently by Harvey et al. (2006) and Zachara,
254 (2007), makes use of the bond valence vector, s_{ij} : a vector parallel to the bond with a magnitude
255 equal to the bond flux. Harvey et al. and Zachara proposed that as long as an atom is expected
256 to lie at the center of its coordination polyhedron, the sum of the bond valence vectors, Δs_i in eqn
257 (12), should be zero.

258
$$\Delta s_i = \sum_j s_{ij} \tag{12}$$

259 In coordination spheres with sufficiently high symmetry such as a trigonally distorted
260 tetrahedron, eqn (12) provides sufficient constraints to determine both the O_t -S- O_t and O_t -S- O_b
261 angles. These are shown in the third column of Table 1. The fourth column in Table 1 shows
262 the observed angles in $K_2S_2O_7$. As the disulfate ion always shows a small additional (as yet
263 unexplained) systematic distortion that breaks the trigonal symmetry (Brown 1980b), the angles
264 shown in Table 1 have been averaged to give trigonal symmetry; the reported O_t -S- O_t angles
265 range from 112.9 to 115.7 and the O_t -S- O_b angles from 101.3 to 105.9. In this example the
266 differences between the two predictions and the observed angles is comparable to the
267 experimental uncertainty of one or two degrees. Like the prediction of bond lengths using eqns
268 (5) and (6), the prediction of angles using eqn (11) or (12) does not depend on knowing the
269 positions of the atoms in space, only on the way in which they are linked by bonds.

270 When Δs_i is found by experiment to deviate from zero, it provides a direct measure of the
271 deviation from the higher symmetry environment. Using eqn (3) it is easily shown that Δs_i
272 points along the direction in which an atom is displaced from the center of its coordination
273 sphere, a result that can be useful in analysing the nature of a distorting constraint, for example
274 when predicting the S- O_b -S angle discussed in Section 7. Before pursuing this calculation it is
275 necessary to review the application of the flux theory to atoms with lone pairs.

276 **The flux theory of lone pairs (non-bonding valence-shell charge)**

277 The assumption that the charge in the valence shell is spherically symmetric still applies
278 to atoms with non-bonding charge (lone pairs)⁴ in its valence shell. Even though the valence

⁴ All non-bonding charge in the valence shell is referred to here as 'lone pairs' as this terminology is simple and familiar. It is not intended to imply that this charge consist of

279 shell retains its spherical symmetry, the bonding or non-bonding function of the charge in the
280 valence shell can be distributed in different ways that do not necessarily observe this symmetry.
281 In some compounds both the bonding charge and lone pairs are arranged within the valence shell
282 with spherical symmetry allowing the bond angles to be calculated in the same way as for the
283 high symmetry coordination environments described in Sections 4 and 5. In this case the lone
284 pair is said to be inactive. In other compounds the bonding and non-bonding charge may appear
285 on opposite sides of the valence shell, with the result that the bonding is asymmetric; one side of
286 the atom forms one or more strong (primary) bonds and the other side forms only weak
287 (secondary) bonds or no bonds at all. In this case the lone pair is said to be stereoactive. The
288 bonding around the oxygen atoms in the sulfate ion is an example of this asymmetric bonding.
289 In the sulfate ion the lone pair is said to be stereoactive, but this distortion is not an intrinsic
290 property of the oxygen atom; it is driven by the environment in which the atom finds itself; an
291 atom with lone pairs is able to form bonds that are much stronger than is permitted by the
292 valence matching rule (eqn (8)) by concentrating its bonding charge in the portion of the valence
293 shell used to form the primary bond(s). In order to preserve the spherical symmetry of the
294 valence shell charge, the non-bonding lone pairs must be moved away from the bond region.
295 The result is the separation of the bonding and lone pair charge into separate sections of the
296 valence shell.

297 Since all anions have lone pairs, whether they are stereoactive or not, it is convenient
298 focus this discussion on anions, specifically on oxygen which forms the bridging bond in the
299 X_2O_7 complexes. The arguments, suitably adapted, apply to other anions besides oxygen, as

identifiable pairs of electrons. The integral charge associated with the non-bonding charge is a consequence of the requirement that atomic valences must be integers.

300 well as to cations containing lone pairs. When the bonding around the anion is regular as found
301 around the oxygen atom in MgO which has the NaCl structure, the bonding and non-bonding
302 functions of the valence shell of oxygen are both spherically distributed, but in the presence of a
303 cation such as S^{6+} that has a bonding strength (+1.5 vu) that is larger than that of the anion (-0.5
304 vu), the bonding and non-bonding functions of oxygen are rearranged so as to ensure that the
305 bonding region of the valence shell contains sufficient bonding charge to match that of the
306 sulfur.

307 Most anions adopt an intermediate configuration between the extremes of having full
308 spherical symmetry, and full stereoactivity with all the bonds appearing on one side of the atom.
309 The Principle of Maximum Symmetry (eqn (1)) implies that the default configuration is the
310 symmetric environment observed when the lone pair is not stereoactive. This arrangement is
311 found when the bonding strength, S_A , of the cation is less than that of the anion, S_B . When S_A is
312 larger than S_B this symmetry is broken, but breaking the symmetry implies the presence of an
313 additional constraint (eqn (2)), namely the need to place more bonding charge (and less of the
314 lone pair charge) in the region of the primary bond. In MgO, where in eqn (8) the ratio $|S_A/S_B|$
315 $0.33/0.50 = 0.67$) is less than 1.0, oxygen adopts regular octahedral coordination, but in the
316 sulfate ion, SO_4^{2-} , where $|S_A/S_B|$ ($1.50/0.50 = 3.0$) is greater than 1.0, the S-O bond can only be
317 formed if three quarters of the oxygen bonding charge (1.50 vu) resides in the region of the bond.
318 The remaining one quarter (0.5 vu) then shares the rest of the valence shell with the lone pairs,
319 and the secondary bonds formed by the oxygen atom must have bond valences (fluxes) of less
320 than 0.5 vu.

321 <Table 2 here>

322 The influence of the lone pair on the geometry can be made quantitative by considering
323 the relative bonding strengths of the cation and anion, as illustrated by the oxides of the cations
324 from the third row of the Periodic Table shown in Table 2. The fifth column of this table shows
325 the ratio, $|S_A/S_B|$, between the bonding strength of the cation and the bonding strength, -0.50 vu,
326 of oxygen. The valence matching rule (eqn (8)) is not obeyed by Na_2O which is why Na_2O is
327 unstable, but it is obeyed by Mg^{2+} , Al^{3+} and Si^{4+} all of whose oxides are stable. The remaining
328 elements, P^{5+} , S^{6+} and Cl^{7+} do not satisfy the valence matching rule, but they can form a stable
329 bond with oxygen if the oxygen lone pairs become stereoactive. These cations use as much of
330 the valence-shell charge of the oxygen as needed to form the primary bond by matching the
331 bonding strength of the cation (S_A in column 4 of Table 2). The rest of the valence shell of the
332 oxygen atom comprises most of the non-bonding lone-pair charge together with the remaining
333 bonding charge which is sufficient to form only weak secondary bonds. The number of primary
334 and secondary bonds is shown in column 7.

335 The degree to which the lone pair can be described as stereoactive increases as the
336 bonding strength of the cation increases. No stereoactivity is seen as long as the cation bonding
337 strength is less than that of oxygen, but once that boundary has been passed, the anion moves
338 off-center in its coordination sphere, producing progressively stronger primary bonds and weaker
339 secondary bonds. The oxygen atom in Al_2O_3 (corundum) is four coordinate, but since the
340 bonding strength of aluminum is 0.57 vu, two primary bonds are formed with bond fluxes of
341 0.57 vu (1.86 \AA) leaving the two secondary bonds with only 0.43 vu of flux (1.97 \AA). The
342 degree of stereoactivity increases as the bonding strength of the cation increases. Once the ratio
343 of the bonding strengths exceeds 2.0 the oxides become unstable and oxyanions are formed

344 instead. In all cases the lone pair is not fully stereoactive and some weak (secondary) bonds
345 are formed in the region primarily occupied by the lone pairs.

346 Where the lone pairs are fully stereoactive no secondary bonds are formed and in cases
347 where there is only one primary bond the anion necessarily terminates the bond network leading
348 to the formation of molecules such as CO₂ and CF₄. Molecules are therefore associated with
349 strong bonds, often regarded as covalent, while crystals are associated with weaker bonds,
350 usually described as ionic.

351 The popular Valence Shell Electron Pair Repulsion (VSEPR) model described by
352 Gillespie and Hargittai, (1991) can be derived by replacing the flux with the corresponding
353 number of valence-shell electron-pairs. By defining bonds in terms of electron pairs the VSEPR
354 model restricts its scope to molecules in which the lone pairs are fully stereoactive, though the
355 model also works for partially stereoactive lone pairs if one ignores the secondary bonds. The
356 flux theory is, however, more general, allowing the degree of stereoactivity to be explored and in
357 many cases predicted as described in Section 7.

358 **Predicting bond angles around atoms with lone pairs**

359 The angles around atoms with lone pairs depend on several factors, namely: the bonding
360 strength of the primary ligands, the atomic valence of the ligand and the steric constraints
361 imposed by the surrounding structure. The degree of stereoactivity can be determined from the
362 value of Δs_i in eqn (12). If the valence shell is spherically symmetric and the lone pairs are fully
363 stereoactive, the vector sum of the fluxes linking the core to the lone pairs should be equal and
364 opposite to the sum of the valence vectors of the bonds, $-\Delta s_i$. In the case of a single lone pair
365 this would be 2.00 vu, but both Harvey et al. (2006) and Zachara (2007) found that Δs_i was

366 typically somewhat less, indicating that the lone pairs were only partially stereoactive.
367 Bickmore et al. (2013) have shown that the principal determinant of the degree of stereoactivity
368 is the bonding strength of the primary bonds, approximated in Fig. 2 (taken from their paper) by
369 the bond valence of the strongest bond plotted along the horizontal axis. This shows that as
370 long as the valence of the primary bond is less than the bonding strength of oxygen (-0.50 vu),
371 the lone pair is not stereoactive, but if it is larger than this, the lone pair becomes increasingly
372 stereoactive with Δs_i , plotted along the vertical axis, following eqn (13), reaching a value of 2.0
373 vu when the cation bonding strength is equal to 2.0 vu.

$$\begin{aligned} 374 \quad |\Delta s_i| &= 0 && \text{for } S_A < 0.5 \text{ vu} \\ 375 \quad |\Delta s_i| &= 1.33(S_A - 0.5) && \text{for } S_A > 0.5 \text{ vu} \end{aligned} \quad (13)$$

376 Eqn (13) places restrictions on the possible bond angles but it is not always possible to
377 predict individual angles exactly. When the lone pairs on oxygen are not stereoactive, the
378 coordination is symmetric and the angles can be derived from the symmetry, but when the lone
379 pairs are stereoactive, the number and directions of the secondary bonds are determined in large
380 measure by the bonding strengths and packing requirements of the remaining atoms in the
381 structure. Fig. 2 shows that when the primary bond has a flux greater than 1.0 vu, eqn (13)
382 gives a reasonable prediction of Δs_i . In this region only one primary bond is possible and the
383 bond angles will depend on how the secondary bonds are disposed. If the primary bond has a
384 flux between 0.5 and 1.0 vu, there may be more than one primary bond, and we expect the bond
385 angle between them to be determined by their relative bond fluxes. However, the solid line in
386 Fig. 2 shows that while eqn (13) is approximately followed in this region there is a wide scatter
387 which suggest that the bond flux is not the only determinant of the bond angle.

388 <Table 3 here>

389 The nature of these other factors can be seen by examining the X-O_b-X angles in the
390 X₂O₇ complexes with X = Si⁴⁺, P⁵⁺, S⁶⁺ or Cl⁷⁺. Since the fluxes of the X-O_b bonds are all the
391 same in these complexes (1.00 vu), the variations in the bridging bond angles ranging from 114
392 to 180 (column 5 in Table 3) cannot be explained by the variation in the strength of the primary
393 bond. The X-O-X angle is found to vary systematically with X, suggesting that the valence of
394 the bonded atom, X, is also responsible for determining the degree of lone pair stereoactivity on
395 the bridging oxygen.

396 Because O_b forms only two bonds, each with a flux of 1.00 vu, there is a simple
397 relationship between the X-O-X bond angle, θ , and the magnitude of the bond valence vector
398 sum, Δs_{θ} , around O_b given by eqn (14).

$$399 \quad |\Delta s_{\theta}| = 2s_{xo} \cos(\theta/2) \quad (14)$$

400 Since $s_{xo} = 1.00$ vu, if θ is known Δs_i can be calculated and vice versa. Fig. 2 shows that when
401 $s_{xo} = 1.0$ vu, Δs_i has a range that extends from zero to 1.0 vu corresponding to θ varying from
402 180 to 120 which, as expected, covers the range of bridging angles shown by the X₂O₇
403 complexes in Table 3.

404 The most obvious factor that correlates with these angles is the valence of the X atom
405 which measures the total charge in the valence shell of X, and hence determines the density of
406 the flux around X. Even though the X-O bond flux does not change, increasing the valence of X
407 concentrates this flux into a smaller solid angle at X, and since the flux lines linking the X and O
408 atoms are continuous, the solid angle of the X-O bond at O must also be reduced. Increasing the
409 density of the bonding charge in the valence shell of O can only be achieved by displacing more

410 of the non-bonding charge from the bond region by making the lone pairs more stereoactive.
411 Silicon has a valence of 4.0 vu so a bond of valence 1.0 vu subtends a solid angle of $4\pi/4 = 3.14$
412 steradians at the silicon nucleus, where 4π is the solid angle of the whole sphere. Chlorine on
413 the other hand has a valence of 7.0 vu so a bond of 1.0 vu occupies a solid angle of just $4\pi/7 =$
414 1.79 steradians at the chlorine nucleus. The smaller the angle at X, the greater the density of the
415 flux in the bond and the smaller the angle at O. Increasing the valence of X thus increases the
416 density of the bonding flux at O leaving less space for the lone pair in the bond region; the lone
417 pair is forced to become more stereoactive and the X-O_b-X angle becomes smaller. If the
418 degree of stereoactivity is given by $|\Delta s_i|/\sqrt{2}$, where the denominator is the value of $|\Delta s_i|$ when the
419 two lone pairs are fully stereoactive, then the degree of stereoactivity shown by the complexes in
420 Table 3 ranges from zero to 77%.

421 This can be made semi-quantitative (Brown 2014a). The bond flux occupies a volume
422 that can be approximated by two outward pointing cones sharing a common base of area A, one
423 with its apex at the X atom subtending an angle Ω_X , the other with its apex at O subtending an
424 angle Ω_O . Since the base area of a cone with height r and apical solid angle Ω is given
425 approximately by eqn (15):

$$426 \quad A = r^2\Omega \quad (15)$$

427 and since the area A is common to both cones, we can write:

$$428 \quad r_X^2\Omega_X = r_O^2\Omega_O$$

429 where r_X and r_O are the distances from X and O respectively to the common area A,

$$430 \quad \text{or} \quad \Omega_O = \Omega_X(r_X/r_O)^2 \quad (16)$$

431 From eqn (10)

432
$$\Omega_X = 4\pi\phi/V_X$$

433 and since ϕ , the flux of the X-O bond, is 1.0 vu it follows that:

434
$$\Omega_O = 4\pi(r_X/r_O)^2/V_X \tag{17}$$

435 The ratio $(r_X/r_O)^2$ is not known, but if the common base of the cones lies at the point where the
436 space occupied by the bond is widest, the ratio is likely to be of the order of 1.0. The value of
437 2.0 gives reasonable agreement with the observed angles. If this value is assumed, the angle
438 subtended by the X-O bond at the oxygen atom is given by eqn (18).

439
$$\Omega_O = 4\pi(2.0/V_X) \tag{18}$$

440 The relationship between θ and the solid angle, Ω , requires a calibration that can be fixed by
441 three high symmetry points; the two extreme cases where the lone pairs are inactive and fully
442 active, and one intermediate point. If the lone pairs are inactive, $\theta = 180^\circ$, $\Omega_O = 4\pi \times 0.5$
443 steradians. If the lone pair is fully stereoactive the bond flux of 1.0 vu occupies 1/6 of the total
444 oxygen valence shell and the oxygen atom's six valence units will be arranged at the corners of
445 an octahedron, in this case $\theta = 90^\circ$, $\Omega_O = 4\pi \times 0.17$ steradians. The intermediate case has
446 triangular symmetry: a lone pair flux of 2 vu points to one corner of the triangle and a
447 combination of 1.0 vu of bonding and 1.0 vu of non-bonding (lone pair) flux each point to the
448 other two corners. For this case $\theta = 120^\circ$ and Ω_O is $4\pi \times 0.33$ steradians. The correlation
449 between θ (in degrees) and V_X , eqn (19), is found by converting Ω_O to V_X using eqn (18).

450
$$\theta = 90 - 90/V_X + 540/V_X^2 \tag{19}$$

451 The angles, θ , predicted by eqn (19) are compared with the observed ranges in the last two
452 columns of Table 3. These angles are used to calculate the values of Δs_i shown in columns 2
453 and 3 using eqn (14). Given the assumptions made in the above analysis, the agreement

454 between the predicted and observed angles is sufficient to suggest that the difference in flux
455 density is the cause of the narrowing of the X-O_b-X angles in going between X = Si⁴⁺ and Cl⁷⁺.

456 The wide range of observed angles for a given X, up to 40° in the case of Si₂O₇⁶⁻, suggests
457 that the angles are affected by other non-intrinsic factors, factors that depend on the context in
458 which the complex is found. These include the steric and packing requirement and must be
459 analyzed separately for each compound. The range of observed bridging angles is largest for
460 the disilicate ion for several reasons, the angle is particularly sensitive to the choice of $(r_X/r_O)^2$ in
461 deriving eqn (19), the flux has a lower density making the bond soft, and the disilicate group,
462 being more tightly bonded to the external structure, is more responsive to the external stresses.
463 As V_X increases, the angles become stiffer and the linkages to the rest of the structure weaker.

464 The above discussion shows that three separate effects affect the angles between the
465 primary bonds formed by atoms with lone pairs. The first is the size of the flux of the X-O
466 bond, the second is the density of this flux and the third is the stress induced by the structure of
467 adjacent atoms.

468 **Bond angles in transition metal complexes**

469 As the concept of a valence shell is not well defined in the transition metals, we must
470 define the valence shell as containing just the bonding charge, relegating any non-bonding
471 charge to the core, even though the core and valence shell may have similar energies.

472 As most transition metals are either four- or six-coordinate, their bond angles can be
473 derived from their tetrahedral or octahedral geometries in the same way as main group cations.
474 There are, however, a few exceptions in which intrinsic electronic instabilities result in bonding
475 geometries in which the expected high symmetry is broken.

476 The largest of these distortions is found around early transition metals in their d^0 and d^1
477 states. When they are in an environment with a center of symmetry they are unstable.
478 Tetrahedral coordination is unaffected as it has no center of symmetry, but when these atoms are
479 six-coordinated, they show a tendency to move away from the center of their coordination
480 sphere, a distortion that becomes larger as one moves across the Periodic Table. It is absent for
481 Sc^{3+} ; small displacements are found in some compounds of Ti^{4+} as for example in $BaTiO_3$, but it
482 may also appear as a disordered displacement in compounds where the titanium atom nominally
483 occupies a site with a crystallographic center of symmetry as in $SrTiO_3$ (Abramov et al. 1995).
484 Around V^{5+} the distortion is much larger and is always present, while six-coordinated Cr^{6+} is
485 unknown, even though the chromium atom could easily surround itself with six oxygen atoms at
486 the expected bond distance. The environment of V^{5+} in V_2O_5 provides a useful case study. The
487 vanadium atom is displaced towards one of the six ligands, giving it a tetragonally distorted
488 octahedral environment of oxygen atoms with the two axial bonds having lengths of 1.59 Å (1.80
489 vu) and 2.80 Å (0.06 vu) and four equatorial bonds of length 1.89 Å (0.80 vu). The large flux of
490 the short bond causes the equatorial bonds to be bent by 14° towards the longer axial bond
491 (Shklover et al. 1996). One can describe this distortion as a displacement of the vanadium atom
492 away from the center of a rigid octahedron of oxygen atoms, but as the discussion in Section 5
493 points out, displacing the atom in a rigid octahedron of ligands will always result in a non-zero
494 valence vector sum pointing in the direction of the displacement. Bending the equatorial bonds
495 away from the shortest bond helps to reduce this sum, but it is not sufficient to keep the sum at
496 zero. Any distortion shown by d^0 and d^1 transition metal cations moving off-center in an
497 octahedral environment implies a polarization of the charge in the valence shell in the direction

498 of the displacement of the vanadium atom. In V_2O_5 the bond valence vector sum is 0.97 vu,
499 indicating a significant polarization, but this appears to be compensated by a corresponding
500 opposite polarization of the core so as to retain a total charge density that is as close as possible
501 to spherical (Gillespie et al. 1996). One could consider the polarization of the valence shell to
502 be an artifact of the way the valence shell has been defined, since a definition that included the
503 polarized non-bonding charge would be closer to maintaining spherical symmetry. Kunz and
504 Brown (1995) were able to predict the variation in the bond lengths in d^0 transition metals by
505 assigning specific capacitances to the bonds in the network equations (eqns (5) and (6)) but so
506 far there has been no attempt to explore either the bond angles or the properties of Δs_i in these
507 complexes.

508 A centrosymmetric tetragonal distortion of octahedral coordination is found around Cu^{2+}
509 and Mn^{3+} , with both axial bonds becoming longer and the equatorial bonds shorter. This is
510 usually called the 'Jahn-Teller' distortion, though the Jahn-Teller theorem is more general,
511 stating that any system will distort if such a distortion can remove a degeneracy in the ground
512 state (Dunitz and Orgel 1960). Since this distortion is centrosymmetric, all the bond angles are
513 fixed at 90° by symmetry. A similar distortion is found around Ni^{2+} and Pt^{2+} where it is
514 sufficiently large that the axial bonds have disappeared and only the four equatorial bonds
515 remain.

516 The late transition metals show a number of unusual bonding features associated with
517 Pearson (1973) softness, but though unusual environments are sometimes found, the bond angles
518 generally remain close to those expected for high symmetry coordination.

519 **Steric strains**

520 The prediction of bond lengths and angles in the flux theory depends only on a
521 knowledge of the bond topology — that is, a knowledge of the way in which the atoms are
522 linked by bonds. There is no guarantee that this geometry can be sustained when the atoms are
523 mapped into three-dimensional space. Some bonds may need to be stretched and others
524 compressed and the bond angles may also have to be strained. Table 3 shows that the Si-O_b-Si
525 angles can be strained by as much as 20 or 30°. Such strains depend on the way in which all the
526 atoms in the structure are packed, making it impossible to predict how the angles will change
527 without a detailed knowledge of the crystal structure. However, the predictions of the bond
528 lengths and angles using the flux theory constitute a reference geometry from which the size of
529 the steric strain can be measured, and a knowledge of this strain allows one to analyse the
530 stresses that occur within a given crystal structure. Further study is needed to reveal how much
531 steric strain the angles can absorb before the structure becomes unstable.

532 **Implications**

533 The electrostatic flux theory provides a physically correct explanation of the bonding that
534 occurs between two atoms with overlapping valence shells. Both the electrostatic flux and the
535 chemical bond depend on the size of the valence charge that forms the bond, but neither of them
536 depends on how that charge is distributed. The result is a physical theory of the bond that is as
537 simple and intuitive as the empirical chemical bond model, while avoiding the traditional
538 language of chemistry that is often more confusing than enlightening. ‘Resonance’ is made
539 redundant by the principle of maximum symmetry (eqn (1)), the distinction between ‘covalent’
540 and ‘ionic’ bonds vanishes before an electrostatic flux that treats all localized bonds equally, and
541 ‘orbitals’ used for calculating charge densities become irrelevant since the flux does not depend

542 on the distribution of the charge.

543 If one knows the chemical formula of a compound, the valence matching rule, eqn (8), is
544 often sufficient to propose a reasonable bond network that can be used with eqns (5) and (6) to
545 predict the lengths of the bonds, and with eqn (11) or (12) to predict the angles between them.
546 In this way one can determine the ideal chemical geometry of the compound from a knowledge
547 of just its formula. The difficult part is mapping this network into three-dimensional space
548 while preserving the ideal geometry. If the network has a high enough symmetry, there are
549 ways in which a matching crystal space group can be found (Brown, 2002), but preserving the
550 chemical geometry during this mapping may not be possible, in which case the bond lengths and
551 angles will be strained. Knowing this strain helps us to understand the stresses involved in the
552 mapping, and may suggest ways in which the strain might be relaxed, for example by lowering
553 the symmetry of the crystal or redistributing the valence among the cations (charge transfer).
554 This can lead to a fuller understanding of the phase diagram and such unusual physical
555 properties as ferroelectricity, colossal magnetoresistance and superconductivity.

556 While the use of the bond valence model in the prediction and analysis of bond lengths is
557 well established, the prediction of bond angles is a new application only now being explored. In
558 this paper I have presented a number of examples to show the potential of the flux theory. It
559 shows promise to extend the VSEPR model to the prediction of the bond angles formed by atoms
560 with lone pairs, even though predicting bond angles around electronically distorted transition
561 metals may prove to be more of a challenge.

562 This study shows that bond angles are determined by the angular distribution of charge
563 densities that remain essentially spherical even when atoms are bonded. The spherical symmetry

564 of the electrostatic field around each atom is responsible for directing all bonds. The presence
565 of lone pairs allows anions to form bonds that are stronger than would otherwise be expected, by
566 concentrating their bonding flux in the region of the strong bonds, leaving other parts of the
567 valence shell with higher concentrations of non-bonding flux. The result is an asymmetric
568 bonding environment. Spherical symmetry around an anion is found only when the bonds are
569 weak. Despite this difference in geometry, all bonds have the same flux character, though this
570 underlying unity is obscured when it is asserted that bonds in asymmetric environments are
571 directed *because* they are covalent and those in symmetric environments are not directed
572 *because* they are ionic. The statement that ‘covalent bonds are directed and ionic bonds are not’
573 might more appropriately be inverted to read ‘the bonds we call ‘covalent’ are the strong primary
574 bonds that are arranged asymmetrically around the anions, while those we call ‘ionic’ are weak
575 and often arranged symmetrically. Directionality has nothing to do with covalency or ionicity;
576 it is more correct and informative to talk of ‘strong’ and ‘weak’ bonds according to the size of
577 their flux, and to describe their coordination as ‘asymmetric’ or ‘symmetric’ rather than
578 ‘directed’ or ‘not directed’.

579 **Acknowledgements**

580 I wish to thank Barry Bickmore for stimulating discussions of the problems discussed in this
581 paper and Matthew Wander for helpful comments on this manuscript

582 **References**

583 Abramov, Yu.A., Zavodnik, V.E., Ivanov, S.A., Brown, I.D., and Tsirelson, V.G. (1995) The
584 Chemical Bond and Atomic Displacements in SrTiO₃ from X-ray Diffraction Analysis. Acta
585 Crystallographica B51, 942-951.

- 586 Bickmore, B.R., Wander, M.C.F., Edwards, J., Maurer, J., Shepherd, D., Meyer, E., Johansen
587 E.J., Frank, R.A., Andros, C., and Davis, M. (2013) Electronic structure effects in the vectorial
588 bond-valence model. *American Mineralogist*, 98, 340-349.
- 589 Brown, I.D. (1980a) A Structural Model for Lewis Acids and Bases. An Analysis of the
590 Structural Chemistry of the Acetate and Trifluoroacetate Ions. *Journal of the Chemical Society,*
591 *Dalton Transactions* 1980, 1118-1123.
- 592 Brown, I.D. (2008b) On the Prediction of Angles in Tetrahedral Complexes and
593 Pseudotetrahedral Complexes with Stereoactive Lone Pairs. *Journal of the American Chemical*
594 *Society*, 102, 2112-2113.
- 595 Brown, I.D. (1988) What Factors Determine Cation Coordination Numbers. *Acta*
596 *Crystallographica B*44, 545-553.
- 597 Brown, I.D. (2002) *The Chemical Bond in Inorganic Chemistry: the Bond Valence Model,*
598 Oxford, Oxford University Press.
- 599 Brown, I.D. (2009) Recent developments in the methods and applications of the bond valence
600 model. *Chemical Reviews* 109, 6858-6919.
- 601 Brown I.D. (2014a) Bond valence theory. In *Bond Valences*, Brown I.D. and Poeppelmeier, K.R.
602 Eds, *Structure and Bonding* 158, 11-58
- 603 Brown, I.D. (2014b) A comprehensive updated listing of bond valence parameters can be found
604 at www.iucr.org/resources/data/datasets/bond-valence-parameters
- 605 Dunitz, J.D., and Orgel, L.E. (1960) Stereochemistry of inorganic solids. *Advances in*
606 *Inorganic Chemistry and Radiochemistry*, 2, 1-160.
- 607 Gibbs, G.V., Hamil, M.M., Louisnathan, S.J., and Bartell, L.S. and Yow, H. (1972) Correlation

608 between Si-O bond length, Si-O-Si angle and bond overlap populations calculated using
609 extended Huckel molecular orbital theory. *American Mineralogist* 57, 1578-1613.

610 Gillespie, R.J., and Hargittai, I. (1991) *The VSEPR Model of Molecular Geometry*. New York,
611 Prentice Hall.

612 Gillespie, R.J., Bytheway I., Tang, T-H., and Bader, R.F.W. (1996) *Geometry of the fluorides,*
613 *oxyfluorides and methanides of vanadium(V), chromium(VI) and molybdenum(VI):*
614 *understanding the geometry of non-VSEPR molecules in terms of core distortion*. *Inorganic*
615 *Chemistry* 35, 3954-3963.

616 Harvey, M.A., Baggio, S, and Baggio, R. (2006) A new simplifying approach to molecular
617 geometry description: the vectorial bond-valence model. *Acta Crystallographica B*62,
618 1038–1042.

619 Kunz, M., and Brown, I.D. (1995) Out-of-center distortions around octahedrally coordinated d^0
620 transition metals. *Journal of Solid State Chemistry*. 115, 395-406.

621 Lynton, H., and Truter, M.R.. (1960) An accurate determination of the crystal structure of
622 potassium pyrosulphate. *Journal of the Chemical Society* 1960, 5112-5118.

623 Murray-Rust, P., Burgi, H-B., and Dunitz, J.D. (1975) *Chemical reaction paths. V. The SN1*
624 *tetrahedral reaction of molecules*. *Journal of the American Chemical Society* 97, 921-923.

625 Pearson, R.G. (1973) *Hard and soft acid and bases*. Stroudberg PA USA: Dowden, Hutchinson
626 and Ross.

627 Shklover, V., Haibach, T., Ried, F., Nesper, R., and Novak, P. (1996) Crystal structure of the
628 product of Mg^{2+} insertion into V_2O_5 single crystals. *Journal of Solid State Chemistry* 123,
629 317-323.

630 Zachara, J. (2007) Novel approach to the concept of bond-valence vectors. Inorganic Chemistry

631 46, 9760–9767.

632

633

634 **Captions**

635 Figure 1 The valence shells (gray) overlap (black) in the bonding region. The flux is shown by
636 the arrows linking the cores (light gray) to the valence shell. The bond is formed by the flux
637 (solid arrows) linking the cores to the overlapping bonding region.

638

639 Figure 2 The relation between the bond valence vector sum shown along the vertical axis
640 labelled $\|S_o\|$, and the valence of the strongest primary bond, shown along the horizontal axis
641 labelled S_{max} , for oxygen atoms. The solid line follows eqn (13). (Reproduced with permission
642 of the American Mineralogical Society from Bickmore et al. 2013).

643

644

645 **Tables**646 Table 1 Angles in degrees in the $S_2O_7^{2-}$ ion.

	Predicted by eqn (11)	Predicted by eqn (12)	Observed (average)
O_t-S-O_t	115.2	116.1	114.1
O_t-S-O_b	103.5	101.5	104.3

647 Notes The observed angles are the trigonally averaged angles found in $K_2S_2O_7$ (Lynton & Truter.
648 1960).

649 Table 2 Oxides of third row elements

Compound	V_A	$\langle N_A \rangle$	S_A vu	$ S_A/S_O $	Stability	N_O^a	Oxygen environment
Na_2O	+1	6.4	+0.16	0.32	deliquescent	8	cubic (CaF_2)
MgO	+2	3.98	+0.33	0.66	stable	6	octahedron (NaCl)
Al_2O_3	+3	5.27	+0.57	1.14	stable	2+2	distorted tetrahedron
SiO_2	+4	4.02	+1	2	stable	2+0	lone pair active
PO_4^{3-}	+5	4.01	+1.25	2.5	oxyanion	1+n	lone pair active
SO_4^{2-}	+6	4	+1.5	3	oxyanion	1+n	lone pair active
ClO_4^-	+7	4	+1.75	3.5	oxyanion	1+n	lone pair active

650 Notes

651 a. Where two values are shown the first refers to the strong primary, the second to the weak
652 secondary bonds. The value of n depends on the nature of the counterion.

- 653 Col. 2: V_A is the valence of the cation,
- 654 Col. 3: $\langle N_A \rangle$ is the average observed coordination number of the cation (Brown 1988)
- 655 Col 4: S_A is the cation bonding strength (Brown 2014a).
- 656 Col 7: N_O is the coordination number of the oxygen.
- 657

658 Table 3. Bridging bond angle in X_2O_7 complexes

	Δs_i predicted from angle (vu)	Δs_i observed (vu)	X-O-X Predicted Eqn 17 (degrees)	X-O-X observed (degrees)
$Si_2O_7^{4-}$	0.00	0.00-0.68	180	140-180
$P_2O_7^{3-}$	0.68	0.42-0.97	140	122-156
$S_2O_7^{2-}$	1.00	0.98-1.09	120	114-121
$Cl_2O_7^-$	1.17	1.07	108	115

659

Figure 1

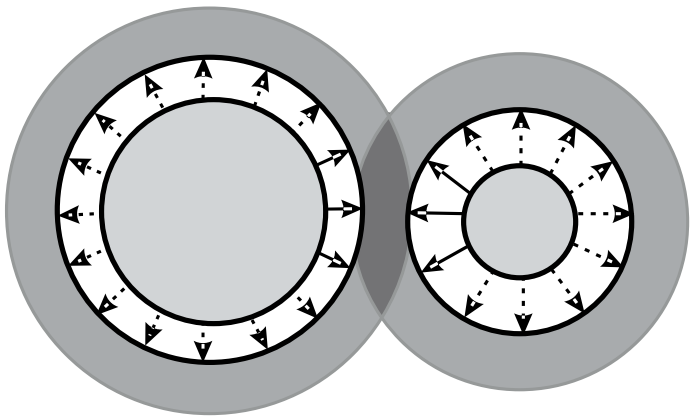


Figure 2

